

AD-A267 512 PAGE

Form Approved
OMB No 0704-0188Public reporting
burden for this
collection of
information is
estimated to
average 1 hour
per response, including the time for reviewing
instructions, searching existing data sources,
gathering the data, reviewing the collection of
information, sending comments regarding this
burden estimate to Washington, DC 20503
and subject to Paperwork Reduction Project (0704-0188)Public reporting
burden for this
collection of
information is
estimated to
average 1 hour
per response, including the time for reviewing
instructions, searching existing data sources,
gathering the data, reviewing the collection of
information, sending comments regarding this
burden estimate to Washington, DC 20503
and subject to Paperwork Reduction Project (0704-0188)

1. AGENCY USE ONLY (Leave blank)		2. REPORT DATE May 1993		3. REPORT TYPE AND DATES COVERED THESIS/DOSSERTATION	
4. TITLE AND SUBTITLE Energy Potential Analysis of Zero Velocity Curves in the Restricted Three-Body Problem				5. FUNDING NUMBERS	
6. AUTHOR(S) Christopher Mark Thomas Tuason					
7. PERFORMING ORGANIZATION NAME(S) AND ADDRESS(ES) AFIT Student Attending: The University of Texas at Austin				8. PERFORMING ORGANIZATION REPORT NUMBER AFIT/CI/CIA- 93-096	
9. SPONSORING/MONITORING AGENCY NAME(S) AND ADDRESS(ES) DEPARTMENT OF THE AIR FORCE AFIT/CI 2950 P STREET WRIGHT-PATTERSON AFB OH 45433-7765				10. SPONSORING/MONITORING AGENCY REPORT NUMBER	
11. SUPPLEMENTARY NOTES					
12a. DISTRIBUTION/AVAILABILITY STATEMENT Approved for Public Release IAW 190-1 Distribution Unlimited MICHAEL M. BRICKER, SMSgt, USAF Chief Administration				12b. DISTRIBUTION CODE	
13. ABSTRACT (Maximum 200 words)					
14. SUBJECT TERMS					
15. NUMBER OF PAGES 53				16. PRICE CODE	
17. SECURITY CLASSIFICATION OF REPORT		18. SECURITY CLASSIFICATION OF THIS PAGE		19. SECURITY CLASSIFICATION OF ABSTRACT	
20. LIMITATION OF ABSTRACT					

DTIC
S
ELECTE
AUG 6 1993
c
D

93-18062



05 110

**ENERGY POTENTIAL ANALYSIS OF
ZERO VELOCITY CURVES
IN THE RESTRICTED
THREE-BODY
PROBLEM**

APPROVED:

Hans Mark
Hans M. Mark

V. Szebehely
Victor G. Szebehely

Wallace T. Fowler
Wallace T. Fowler

DTIC QUALITY INSPECTED 3

Accession For	
NTIS CRA&I	<input checked="" type="checkbox"/>
DTIC TAB	<input type="checkbox"/>
Unannounced	<input type="checkbox"/>
Justification	
By	
Distribution /	
Availability Codes	
Dist	Avail and/or Special
A-1	

Copyright

by

Christopher Mark Thomas Tuason

1993

for my wife and daughter

**ENERGY POTENTIAL ANALYSIS OF
ZERO VELOCITY CURVES
IN THE RESTRICTED
THREE-BODY
PROBLEM**

by

CHRISTOPHER MARK THOMAS TUASON, B.S.E.E.

THESIS

Presented to the Faculty of the Graduate School of
The University of Texas at Austin
in Partial Fulfillment of the
Requirements for the
Degree of
MASTER OF SCIENCE IN ENGINEERING

THE UNIVERSITY OF TEXAS AT AUSTIN

May, 1993

Acknowledgments

I am indebted to all of the faculty and staff whom I have encountered at The University of Texas at Austin. My horizons have expanded in many dimensions by assimilating the philosophy of excellent professors such as Dr. Hans Mark, Dr. Victor Szebehely, and Dr. Wally Fowler, to name three. I wish to thank all of the students who have given me help whenever I needed it. I would also like to thank Dr. E. Zachary Crues for introducing me to the HiQ graphics program for the Macintosh.

This research would not have been possible without support from the Air Force Institute of Technology.

CHRISTOPHER MARK THOMAS TUASON

The University of Texas at Austin

May, 1993

Abstract

ENERGY POTENTIAL ANALYSIS OF ZERO VELOCITY CURVES IN THE RESTRICTED THREE-BODY PROBLEM

by

Christopher Mark Thomas Tuason, B.S.E.E.

Supervising Professor: Dr. Hans M. Mark

The restricted problem of three bodies is a more tractable case than the general three-body problem. Two primary celestial bodies are restricted to a circular orbit while a third body of negligible mass orbits in the plane of motion established by the primaries. Among many other practical applications, these restrictions form a rough approximation to the Earth-Moon-spacecraft problem. This study analyzes the restricted problem by superposition of the energy potential wells that arise from the gravitational and inertial forces of the primaries in their circular motion. Three-dimensional computer graphics are used to illustrate the surfaces that are created by the potentials of the primaries. Zero

velocity curves, also known as Hill's curves, describe the boundary between regions of possible motion and forbidden regions for the third body. These curves are the principle qualitative aspect of the restricted problem. A curve of zero velocity is found by taking a cross-section of the potential surface at a specific energy level corresponding to the Jacobian constant of the third body. The topology of a zero velocity curve may change depending on the energy of the third body. The Lagrange equilibrium points are clearly shown to be located at the critical energy levels where the topology of the zero velocity curves change. The superposition analysis in a three-dimensional representation clearly reveals the component forces involved in the restricted problem and provide a visual model for understanding the stability of motion near the equilibrium points.

Table of Contents

List of Figures	ix
Chapter 1 Introduction	1
Chapter 2 Formulation of the Restricted Problem.....	3
2.1 The Intractable Nature of the Three-Body Problem	3
2.2 Justification for the Restricted Problem	5
2.3 Definition of the Restricted Problem	6
2.4 Equations of Motion	8
2.5 Equations of Motion in the Rotating Frame	10
2.4 Equations of Motion in Dimensionless Coordinates	11
Chapter 3 Energy Potentials.....	16
3.1 The Potential Function.....	16
3.2 An Example of Gravitational Force.....	17
3.3 Kinetic Energy as the Potential of Inertial Force.....	19
3.4 Conservation of Energy	20
3.5 Two-Body Orbit Analysis.....	22
3.6 Superposition of Gravitational Potentials	25
Chapter 4 Derivation of the Potential Function	29
4.1 Characteristics in a Rotating Reference Frame	29
4.2 The Centrifugal Potential.....	32
4.3 Superposition of Potentials	33
Chapter 5 The Equilibrium Points and Zero Velocity Curves.....	38
5.1 The Equilibrium Points.....	39
5.2 Zero Velocity Curves.....	40
5.3 Extreme Values of the Mass Parameter	45
5.4 Applications for the Earth-Moon System	46

Chapter 6 Summary	49
Bibliography	51
Vita	

List of Figures

Figure 2.1	The general problem of three bodies	3
Figure 2.2	The restricted problem, fixed and rotating coordinates	9
Figure 2.3	The restricted problem in non-dimensional coordinates	11
Figure 2.4	Curves of zero velocity for $\mu=0.3$	15
Figure 3.1	Gravitational force field and corresponding potential function.....	18
Figure 3.2	Kinetic energy superimposed on the gravitational potential	23
Figure 3.3	Moon superpositioned on the Earth's gravitational potential	26
Figure 3.4	Sun's potential superpositioned on the Earth-Moon system	27
Figure 4.1	Relationship of forces between inertial and rotating reference	30
Figure 4.2	Centrifugal force and the corresponding potential	32
Figure 4.3	Superposition of primary gravity wells	34
Figure 4.4	Superposition of gravitational with centrifugal potential	35
Figure 5.2	The location of the collinear and equilateral Lagrange points	39
Figure 5.11	Zero velocity curve for $\mu=0.5$	44
Figure 5.12	Zero velocity curve for $\mu=0$, the two-body problem	45
Figure 5.13	The cis-lunar Lagrange point ($\mu=0.0121$).....	46
Figure 5.14	The trans-lunar Lagrange point ($\mu=0.0121$).	47

Chapter 1

Introduction

Sir Isaac Newton published *Philosophiae Naturalis Principia Mathematica* in 1687. Investigating the motion of the Earth, Moon and Sun, he found the problem of three bodies to be extremely challenging. The solutions to the orbits of two bodies were expressed by the simple equations of conic sections. No such solution was found for the three-body problem. He complained that the problem gave him headaches and kept him awake.

The restricted problem of three bodies dates back to Euler, who proposed the use of a rotating coordinate system in 1772, to simplify his second lunar theory. In that year, Lagrange found particular solutions to the restricted problem, showing the existence of equilibrium points.

Laplace attempted to prove the stability of the solar system in 1773, by using a perturbation technique that solved for the first-order deviation from a two-body orbit. Poisson continued with a series expansion to solve for higher order terms. Then in 1899, J. Henri Poincaré proved that such series solutions are not convergent in general. Concentrating on the three-body problem, he established the concept of non-integrable dynamical systems.

Because of the absence of analytical solutions, qualitative methods are indispensable to the study of the non-integrable restricted three-body problem. In 1836, Jacobi presented an integral to the equations of motion for the restricted problem that gives a constant to associate the speed of the third body with its

position. Hill, in 1878, applied the Jacobian constant to define regions of possible motion and regions where motion is prohibited, separated by curves of zero velocity. These curves are the principle qualitative aspect of the restricted problem.

Zero velocity curves are given a thorough analysis in the available literature, some of which is listed in the references. The purpose of this paper is to use three-dimensional graphics to help give a comprehensive explanation for the significance of zero velocity curves. The energy potential analysis is intended to give a conceptual understanding of the restricted three-body problem.

The problem is defined and equations of motion are derived in chapter 2. Zero velocity curves are introduced as a qualitative method of gaining information about the motion without actually solving the differential equations. Chapter 3 reviews the relationship between a force function and a potential function in preparation for the superposition analysis of the zero velocity potential surface in chapter 4. The Lagrange equilibrium points are shown to be special points of zero gradient for the surface in chapter 5. Zero velocity curves are shown to be obtained from the intersection of the potential at the energy level specified by the Jacobian constant. Finally, the significance of this research is emphasized with applications to future plans for space exploration.

Chapter 2

Formulation of the Restricted Problem

2.1 The Intractable Nature of the Three-Body Problem

For anyone who has learned the elegant geometry of the solutions to the two-body problem, it is not at all obvious that the introduction of a third body will cause such complications. As disclosed by Poincaré in *Méthodes Nouvelles* of 1899, dynamical systems of more than two bodies are non-integrable. Although a particular solution may be found under special conditions, no generally valid analytical solutions exist for the three-body problem. To understand the need for the restricted formulation, a brief discussion of the general problem follows.

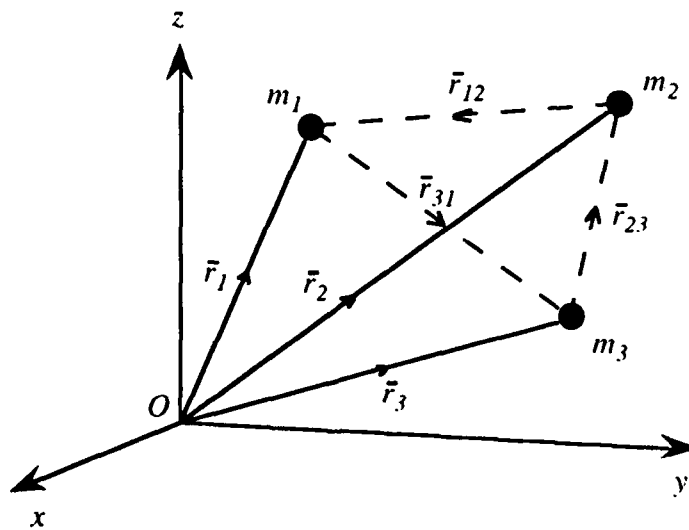


Figure 2.1 The general problem of three bodies is an eighteenth-order dynamical system consisting of three second-order differential equations in three dimensions.

The general problem of three bodies states that three masses are mutually attracted according to the law of Newtonian gravitation. This forms the dynamic system depicted in figure 3.1. The three second-order differential equations in three dimensions form an eighteenth-order dynamical system:

$$\begin{aligned}
 m_1 \ddot{\vec{r}}_1 &= -\frac{Gm_1m_2}{r_{12}^2} \hat{r}_{12} + \frac{Gm_3m_1}{r_{31}^2} \hat{r}_{31}, \\
 m_2 \ddot{\vec{r}}_2 &= -\frac{Gm_2m_3}{r_{23}^2} \hat{r}_{23} + \frac{Gm_1m_2}{r_{12}^2} \hat{r}_{12}, \\
 m_3 \ddot{\vec{r}}_3 &= -\frac{Gm_3m_1}{r_{31}^2} \hat{r}_{31} + \frac{Gm_2m_3}{r_{23}^2} \hat{r}_{23},
 \end{aligned} \tag{2.1}$$

where G denotes the universal gravitational constant. The masses of the three bodies are m_1 , m_2 , and m_3 , their position vectors are $\vec{r}_1(x,y,z)$, $\vec{r}_2(x,y,z)$, and $\vec{r}_3(x,y,z)$ and the dots denote time derivatives. Two vectors connect each mass along the line of gravitational force and are given by:

$$\vec{r}_{12} = \vec{r}_1 - \vec{r}_2, \quad \vec{r}_{23} = \vec{r}_2 - \vec{r}_3, \quad \vec{r}_{31} = \vec{r}_3 - \vec{r}_1, \tag{2.2}$$

with magnitudes r_{ij} and unit vectors \hat{r}_{ij} .

A far cry from the lucidity of conic sections, a third body creates tangled trajectories in three-dimensions governed by these daunting equations of motion. Through the use of integrals from conservation of linear and angular momentum, conservation of energy, and the removal of time dependence, the eighteenth-order

system can be reduced to a sixth-order system. Because there are no external forces, the center of mass of the system travels on a straight line with constant velocity. These two vector equations give six constants thereby reducing the eighteenth-order system to twelve. Conservation of angular momentum gives one vector equation with three constants of integration, further reducing the system to ninth-order. Conservation of energy is a scalar relationship that brings the order down to eight.

Further reduction requires sacrifice of important information. With much effort, it is possible to eliminate time from the equations, leaving a sixth-order system to describe only the geometry of the motion. After these great strides, the remaining sixth-order differential equation is still unwieldy [15].

2.2 Justification for the Restricted Problem

Upon reaching this analytical dead end in the general problem, any simplifying assumptions are enthusiastically considered. Judging which assumptions are acceptable can be a difficult task. Fortunately, nature itself provides the simplifications. Despite the many-body situation of the real world, predictable two-body orbits dominate much of the observed motion of the universe. It is most likely due to the instabilities of three (or more) bodies that well-ordered systems evolve. Research indicates that whenever three bodies of like magnitude interact, one of the bodies will eventually get ejected while the other two form a stable binary [17].

Stable two-body motion takes place on many levels of scale. A spacecraft orbits around the Moon. The Moon orbits around the Earth. The Earth orbits around the Sun. The Sun orbits around the core of the Milky Way. The galactic core, probably a black hole, may be in orbit around some center of the universe. At every level of this self-similar structure reminiscent of fractal geometry, the mass-distance ratios are established so that motion is directed by, at most, two dominating gravitational sources of similar magnitude.

Although numerous masses are found in our solar system, it is an easy task to identify two masses whose interaction can be approximated by two-body motion, while the presence of other masses merely serve to perturb the orbit. These systems are often found to have elliptical orbits of low eccentricity. When the masses of the strongly interacting members are much greater than a third body being considered, the situation is ripe for simplifying assumptions to make the three-body problem more tractable.

It has long been known that the Earth-Moon system forms such a binary of near circular motion. The history of the restricted three-body problem is over 200 years old, being formulated by Euler in his second lunar theory. In his *Theoria Motuum Lunae*, published in 1772, he suggests using a reference frame that rotates with the system so that the positions of the Earth and Moon are fixed.

2.3 Definition of the Restricted Problem

The restricted three-body problem is set up as a degenerate case of the general problem. Generally, the motion of each body is influenced by the

gravitational attraction from each of the other masses. In the situation where a third body is of a much smaller mass than the other two, the third body has a very small effect on the motion of the larger masses. The two larger masses, referred to as the primaries, act as a pair that has their motion approximated by a two-body problem with their trajectories predetermined. The motion of the third body, as affected by the two primaries, is the subject of the restricted three-body problem. As in the general problem, the mass distributions of all bodies are such that they may be treated as point masses. In considering only the motion of the third body, only the last of equations (2.1) is necessary. Being left with a single second-order differential equation in three dimensions, the eighteenth-order system is restricted to six.

It is possible to evaluate different geometries for the primaries. For example, much analytical and numerical work has been done on the elliptical three body problem [15]. This study will deal with the most basic formulation in which the primaries are in a circular orbit and the initial conditions of the third body are such that its motion will remain in the same plane of motion with the primaries. These conditions are explicitly termed the *coplanar circular restricted three-body problem*.

As opposed to the three-dimensional restricted problem, the coplanar constraint produces equations of motion that are fourth-order. A disadvantage of the restricted formulation is that ten of the integrals that were used to reduce the general problem are no longer available. For instance, conservation of energy was discarded by neglecting the small effect that the third body had on the motion of the primaries. The only known integral for the restricted problem was discovered

by Jacobi in 1836, and gives a constant that also bears his name. The Jacobian constant connects the speed of the third body to its position through the potential function.

2.4 Equations of Motion

The notation that is used follows Szebehely, 1967 [15]. The equations of motion are greatly simplified by a clever choice of coordinate axes. With the primaries in circular orbit, their barycenter is chosen for the origin and the \bar{x} axis coincident with their line of syzygies so that the masses m_1 and m_2 remain fixed in the rotating reference frame. Mass m_1 is chosen as the larger of the two and is fixed at $(b,0)$. The smaller mass m_2 is fixed at $(-a,0)$. The barycentric relation is such that $m_1b = m_2a$, where $a \geq b$ because $m_1 \geq m_2$. The circular orbit requires that gravitational force is balanced by centrifugal force so that:

$$\frac{Gm_1m_2}{(a+b)^2} = m_1bn^2 = m_2an^2. \quad (2.3)$$

The symbol G is the gravitational constant and the mean motion n is their average angular velocity. The rotating frame is displaced from the inertial frame by an angle nt^* , which is the longitude of m_1 . The symbol t^* represents time. Notice that clean variable names are being reserved for the non-dimensional representation.

By defining l as the total distance between the primaries, Kepler's third law is derived from Newton's force law shown in equation (2.3) above:

$$Gm_1 = al^2n^2, \quad Gm_2 = bl^2n^2,$$

$$G(m_1 + m_2) = l^3n^2. \quad (2.4)$$

The equations of motion in the inertial frame of reference are:

$$\begin{aligned} \frac{d^2X}{dt^{*2}} &= -\frac{Gm_1}{R_1^3}(X - b\cos nt^*) - \frac{Gm_2}{R_2^3}(X + a\cos nt^*), \\ \frac{d^2Y}{dt^{*2}} &= -\frac{Gm_1}{R_1^3}(Y - b\sin nt^*) - \frac{Gm_2}{R_2^3}(Y + a\sin nt^*), \end{aligned} \quad (2.5)$$

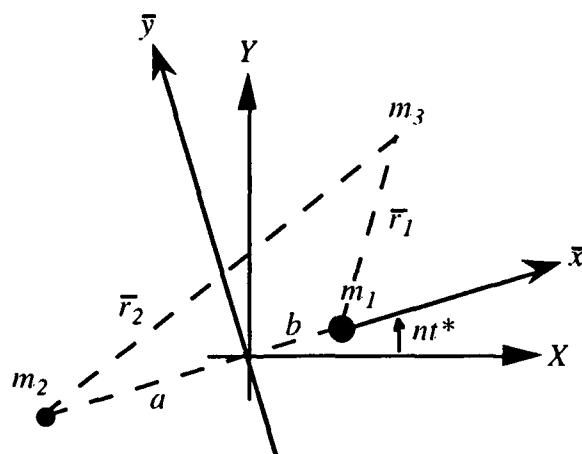


Figure 2.2 The restricted three-body problem showing the relationship between fixed and rotating coordinate systems.

and may be compared to equation (2.1) of the general problem. The distances R_1 and R_2 are:

$$\begin{aligned} R_1 &= \sqrt{(X - b \cos nt^*)^2 + (Y - b \sin nt^*)^2}, \\ R_2 &= \sqrt{(X + a \cos nt^*)^2 + (Y + a \sin nt^*)^2}. \end{aligned} \quad (2.6)$$

2.5 Equations of Motion in the Rotating Frame

With the aim of simplifying the equations of motion, the coordinates are transformed to the rotating system. Complex variables are a convenient method to carry out this operation. Let the inertial frame be described by the complex variable $Z = X + iY$, and the rotating frame by the complex variable $z = \bar{x} + i\bar{y}$. Where X , Y , \bar{x} and \bar{y} are all real scalars. Then the coordinate transformation by a rotation through angle nt^* is given by

$$Z = ze^{int^*}. \quad (2.7)$$

The first derivative of Z with respect to time is

$$\frac{dZ}{dt^*} = inze^{int^*} + e^{int^*} \frac{dz}{dt^*}, \quad (2.8)$$

and the second derivative is

$$\begin{aligned} \frac{d^2Z}{dt^{*2}} &= \left((in)^2 ze^{int^*} + ine^{int^*} \frac{dz}{dt^*} \right) + \left(e^{int^*} \frac{d^2z}{dt^{*2}} + ine^{int^*} \frac{dz}{dt^*} \right) \\ &= \left(\frac{d^2z}{dt^{*2}} + 2in \frac{dz}{dt^*} - n^2 z \right) e^{int^*} \end{aligned} \quad (2.9)$$

Applying this result to equations (2.5), the complex form for the equations of motion is

$$\frac{d^2 z}{dt^{*2}} + 2in \frac{dz}{dt^*} - n^2 z = -\frac{Gm_1(z-b)}{\bar{r}_1^3} - \frac{Gm_2(z+a)}{\bar{r}_2^3}, \quad (2.10)$$

which, when separated into the real and imaginary components, gives

$$\frac{d^2 \bar{x}}{dt^{*2}} - 2n \frac{d\bar{y}}{dt^*} - n^2 \bar{x} = -\frac{Gm_1(\bar{x}-b)}{\bar{r}_1^3} - \frac{Gm_2(\bar{x}+a)}{\bar{r}_2^3}, \quad (2.11)$$

$$\frac{d^2 \bar{y}}{dt^{*2}} + 2n \frac{d\bar{x}}{dt^*} - n^2 \bar{y} = -\frac{Gm_1 \bar{y}}{\bar{r}_1^3} - \frac{Gm_2 \bar{y}}{\bar{r}_2^3},$$

where:

$$\bar{r}_1 = \sqrt{(\bar{x}-b)^2 + \bar{y}^2}, \quad \bar{r}_2 = \sqrt{(\bar{x}+a)^2 + \bar{y}^2}. \quad (2.12)$$

2.4 Equations of Motion in Dimensionless Coordinates

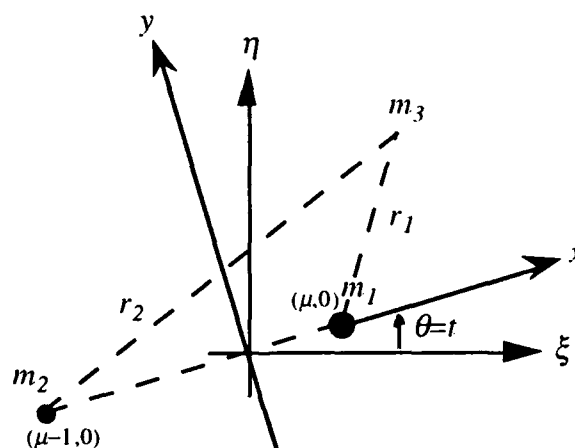


Figure 2.3 Restricted three-body problem in non-dimensional coordinates

The physical parameters that appear in equation (2.11) are related by the following equations and can be replaced by a single parameter through the conversion to dimensionless coordinates:

$$\begin{aligned} x &= \frac{\bar{x}}{l}, & y &= \frac{\bar{y}}{l}, & r_1 &= \frac{\bar{r}_1}{l}, & r_2 &= \frac{\bar{r}_2}{l}, \\ m_1 b &= m_2 a, & a + b &= l, & t &= nt^*, \end{aligned} \quad (2.13)$$

$$\mu_2 = \frac{m_2}{m_1 + m_2} = \frac{b}{l}, \quad \mu_1 = \frac{m_1}{m_1 + m_2} = \frac{a}{l}.$$

Substitution into equations (2.11) gives the results:

$$\begin{aligned} \ddot{x} - 2\dot{y} - x &= - \left[\frac{\mu_1(x - \mu_2)}{r_1^3} + \frac{\mu_2(x + \mu_1)}{r_2^3} \right], \\ \ddot{y} + 2\dot{x} - y &= - \left[\frac{\mu_1 y}{r_1^3} + \frac{\mu_2 y}{r_2^3} \right], \end{aligned} \quad (2.14)$$

where an identity form of Kepler's third law has also been used to eliminate G .

These equations may be written in a compact form by moving the x and y terms to the right hand side and defining the potential function $\bar{\Omega}$:

$$\begin{aligned} \ddot{x} - 2\dot{y} &= \frac{\partial \bar{\Omega}}{\partial x} = x - \left[\frac{\mu_1(x - \mu_2)}{r_1^3} + \frac{\mu_2(x + \mu_1)}{r_2^3} \right], \\ \ddot{y} + 2\dot{x} &= \frac{\partial \bar{\Omega}}{\partial y} = y - \left[\frac{\mu_1 y}{r_1^3} + \frac{\mu_2 y}{r_2^3} \right]. \end{aligned} \quad (2.15)$$

The potential function $\overline{\Omega}$ will be comprehensively derived in chapter 4, but for continuity, it is given to be

$$\overline{\Omega} = \frac{1}{2}(x^2 + y^2) + \frac{\mu_1}{r_1} + \frac{\mu_2}{r_2}, \quad (2.16)$$

with distances

$$\begin{aligned} r_1 &= \sqrt{(x - \mu_2)^2 + y^2}, \\ r_2 &= \sqrt{(x + \mu_1)^2 + y^2}. \end{aligned} \quad (2.17)$$

Notice that equations (2.15), (2.16) and (2.17) can be expressed as a function of the single parameter

$$\mu \equiv \mu_2 = \frac{m_2}{m_1 + m_2} = \frac{m_1 + m_2 - m_1}{m_1 + m_2} = 1 - \mu_1. \quad (2.18)$$

A constant may be added to the potential function $\overline{\Omega}$ without changing the equations of motion given by equations (2.15). It is sometimes desired to define the potential in a more symmetric form, where

$$\Omega = \overline{\Omega} + \frac{1}{2}\mu_1\mu_2, \quad (2.19)$$

giving

$$\Omega = \frac{1}{2}(\mu_1 r_1^2 + \mu_2 r_2^2) + \frac{\mu_1}{r_1} + \frac{\mu_2}{r_2}. \quad (2.20)$$

The equations of motion are

$$\begin{aligned}\ddot{x} - 2\dot{y} &= \frac{\partial \Omega}{\partial x}, \\ \ddot{y} + 2\dot{x} &= \frac{\partial \Omega}{\partial y}.\end{aligned}\tag{2.21}$$

Jacobi's integral connects the relative speed of the third body to its location as limited by the potential function through the equation

$$V^2 = 2\Omega - C,\tag{2.22}$$

or

$$\dot{x}^2 + \dot{y}^2 = x^2 + y^2 + \frac{2(1-\mu)}{r_1} + \frac{2\mu}{r_2} - C,\tag{2.23}$$

where V is the magnitude of the velocity vector and C is the Jacobian constant.

The most definitive qualitative statement that can be made with the Jacobian integral is to define regions of possible motion and regions from which the third body is forbidden. The boundary between such regions occurs when the velocity of the third body goes to zero. Setting \dot{x} and \dot{y} to zero, equation (2.23) becomes

$$x^2 + y^2 + \frac{2(1-\mu)}{r_1} + \frac{2\mu}{r_2} = C,\tag{2.24}$$

where the Jacobian constant is determined from initial conditions.

This function of position defines a curve of zero velocity for any particular value of the Jacobian constant. Figure 2.4 is a plot of various values of C for the mass parameter $\mu=0.3$.

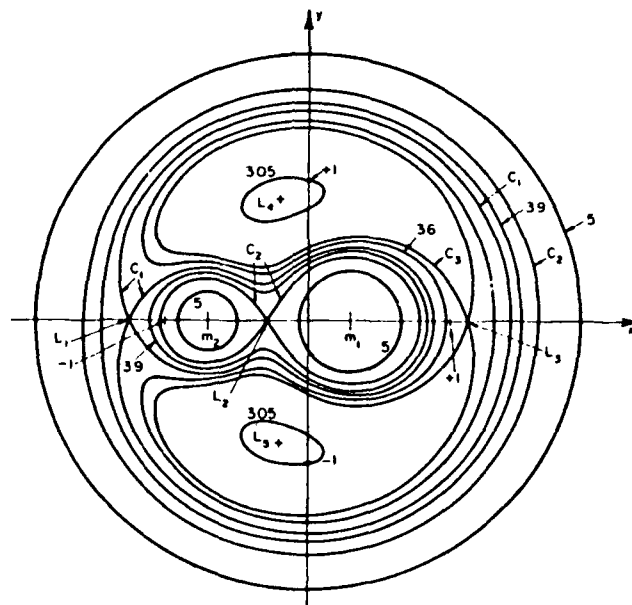


Figure 2.4 Curves of zero velocity for $\mu=0.3$. (reproduced from Szebehely, 1967).

The origin of the potential function and the meaning of zero velocity curves with their equilibrium points are to be explained thoroughly in chapter 5.

Chapter 3

Energy Potentials

3.1 The Potential Function

A vector function can be related by a one-to-one mapping to a scalar function. Such is the connection between a force function to a potential function. The scalar potential function U is generated by integrating the force field \vec{F} along the path $d\vec{r}$:

$$-\int \vec{F} \cdot d\vec{r} = U, \quad (3.1)$$

with the negative sign imposed as a matter of convention. To determine the force at any particular point on the generated potential function, the inverse relationship

$$\vec{F} = -\frac{\partial U}{\partial x} \hat{i} - \frac{\partial U}{\partial y} \hat{j} - \frac{\partial U}{\partial z} \hat{k} = -\vec{\nabla} U, \quad (3.2)$$

is applied, stating that force equals minus the gradient of the potential. Not all force fields have a realizable potential function associated with them. If the vector field has any rotation where $\text{curl } \vec{F} \neq 0$, the value of the integral in equation (3.1) would be dependent upon the path that is taken. To insure path independence, the condition:

$$\frac{\partial^2 F}{\partial x \partial y} = \frac{\partial^2 F}{\partial y \partial x}, \quad (3.3)$$

must hold, thereby ensuring the existence of a potential function. This criterion may also be expressed as the line integral along a simple closed curve in the vector field being equal to zero:

$$\oint \vec{F} \cdot d\vec{r} = 0, \quad (3.4)$$

for any arbitrary closed path in the vector field \vec{F} . Forces that meet this criteria are said to be conservative.

The potential function U may be defined with the addition of an arbitrary constant of integration. The zero energy reference may be chosen at any level by selection of this constant.

3.2 An Example of Gravitational Force

The potential associated with the gravitational force field is obtained by integrating Newton's force law as per equation (3.1) and meets the conservative force criteria of equation (3.3):

$$\begin{aligned} \vec{F}_{grav} = \frac{-Gm_1m_2}{r^2} \hat{r} & \Leftrightarrow U_{grav} = - \int \frac{-Gm_1m_2}{r^2} \hat{r} \cdot d\vec{r} \\ & = Gm_1m_2 \int \frac{1}{r^2} dr \\ & = -\frac{Gm_1m_2}{r} + C, \end{aligned} \quad (3.5)$$

where G is the universal gravitation constant, \hat{r} is the unit vector that points from mass m_1 to mass m_2 , r is the distance between the masses, and C is a constant of integration that is chosen to be zero.

A convenient conceptual model of the resultant potential surface is to think of free space in two dimensions as a stretched sheet of flat rubber. A mass placed on this sheet deforms the rubber and forms a well of potential energy that must be climbed out of in order to move away from the mass. The zero energy reference is chosen to be at the level of the unstretched sheet prior to the introduction of the mass. Once the warping of the sheet is accomplished, zero gravitational potential energy can only be found at an infinite distance from the mass. Figure 3.1 illustrates the mapping of a gravitational force vector field in two dimensions to its corresponding potential surface.

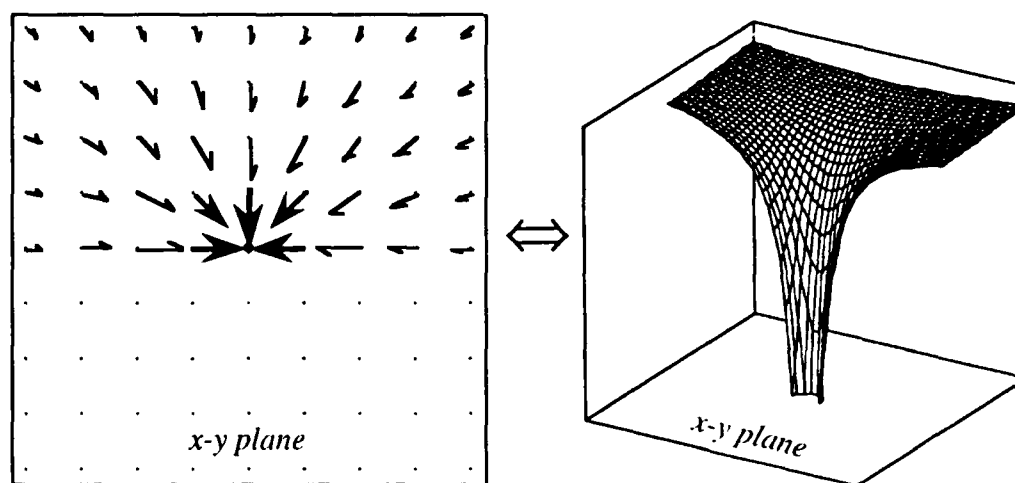


Figure 3.1 Gravitational force field and corresponding potential function. Note that the gradient at any point on the potential surface is the negative force vector in the x - y plane. The z -axis of the potential function is energy. Half of the field has been cut away for clarity.

Notice how the maximum slope at any point on the potential surface corresponds to the magnitude of force at that point. The direction of that gradient is opposite the direction of the force vector. Thus, the scalar potential function has a one-to-one correspondence with the original force function.

3.3 Kinetic Energy as the Potential of Inertial Force

The force and energy potential relationship given by equation (3.2) may be written, for simplicity, in one dimension as:

$$F(x) = -\frac{dU(x)}{dx}. \quad (3.6)$$

When applied to kinetic energy, this yields an intriguing analysis. After some manipulation, it is shown that kinetic energy is the potential of inertial force:

$$\begin{aligned} -\frac{d}{dx}\left(\frac{1}{2}mv^2\right) &= -\frac{d}{dx}\left(\frac{1}{2}m\frac{dx}{dt}\cdot\frac{dx}{dt}\right) = -\frac{1}{2}m\left[\frac{dx}{dt}\cdot\frac{d}{dx}\left(\frac{dx}{dt}\right) + \frac{d}{dx}\left(\frac{dx}{dt}\right)\cdot\frac{dx}{dt}\right] \\ &= -\frac{1}{2}m\left[2\frac{dx}{dt}\cdot\frac{d}{dx}\left(\frac{dx}{dt}\right)\right] = -m\frac{d}{dt}\left(\frac{dx}{dt}\right) = -m\frac{d^2x}{dt^2} = -ma. \end{aligned} \quad (3.7)$$

D'Alembert (1717-1783) suggested that any dynamic system can be described by the equations of statics by introducing inertia as a force. The final term in equation (3.7), $-ma$, is the inertial force of D'Alembert's principle. The negative sign is due to the fact that inertial force opposes the net acceleration that

is experienced by a mass. More on D'Alembert's principle can be found in Torby [18].

3.4 Conservation of Energy

It can be a lengthy process to derive the principle of conservation of energy. Starting with Newton's second law, it is possible to derive the Lagrangian. From the Lagrangian, the Hamiltonian is derived. Imbedded in the Hamiltonian is the time-invariance of energy. It is perhaps difficult to get a good appreciation for the reason why energy should be conserved. However, using the energy potential concept, a direct route proves the energy conservation principle in a manner whose simplicity is intuitively appealing.

For this derivation, Newton's third law is used with D'Alembert's principle and the potential relation of equation (3.1). D'Alembert's principle of inertial force follows directly from Newton's second law. The net acceleration on a body is produced by the sum of external forces through the relation:

$$\sum \bar{F}_{ext} = m\bar{a}, \quad (3.8)$$

$$\sum \bar{F}_{ext} - m\bar{a} = 0, \quad (3.9)$$

$$\sum \bar{F}_{ext} + \bar{F}_{iner} = 0, \quad (3.10)$$

where inertial force is $-m\bar{a}$, as stated in equation (3.7).

Newton's third law states that for every action, there is an equal and opposite reaction. When a force is applied to a body, the acceleration is opposed by inertial force. So the third law is expressed as the sum of all forces equaling zero:

$$\sum_{all} \bar{F} = 0. \quad (3.11)$$

Equation (3.11) looks deceptively like a statics equation and one may wonder how any motion can exist at all. This is explained by the fact that inertial force arising from kinetic energy does not act externally to a body. This matter gets somewhat more complicated when dealing with accelerating frames of reference because in those cases, inertia only acts partially as an internal force. The internal component of inertia is always bound in the kinetic energy of the body's motion relative to the reference frame, whether or not that frame is accelerating. The problem of accelerating reference frames will be addressed more closely in chapter 4.

Applying the relationship given by equation (3.1) to Newton's third law in the form of equation (3.11) and passing the summation inside the integral, the elegant result:

$$\sum_{all} U = - \int \sum_{all} \bar{F} \cdot d\bar{r} = - \int 0 \cdot d\bar{r} = Const, \quad (3.12)$$

where the constant arises from the integration and may be chosen arbitrarily. Therefore, the zero energy reference may be set at any level. This shows that when kinetic energy is treated as inertial potential, conservation of energy follows

directly from Newton's third law and helps to explain *why* energy is conserved. Energy is conserved because every force is opposed by an equal and opposite force.

3.5 Two-Body Orbit Analysis

To understand the significance of the energy potential representation of the restricted three-body problem, it is helpful to first transform a familiar problem to its potential form. The two-body problem provides a simple example. Two-body trajectories follow the geometry of the well-known conic sections. Depending on the energy of the system, the trajectory may follow a circular, elliptical, parabolic, or hyperbolic path. If the total energy is negative, the orbit will be circular or elliptical and the two bodies will remain at a finite distance to each other. For a system with exactly zero total energy, the motion will follow a parabolic orbit with the relative velocity going to zero at infinite distance. When the two-body system has a positive total energy, the orbit is hyperbolic and the two masses depart at a velocity that asymptotically approaches the velocity associated with the kinetic energy of the positive system total. This departure velocity is termed hyperbolic excess velocity.

In the case where the mass of one body is negligible compared to the other, such as a satellite orbiting a planet, the gravitational potential is determined by the large mass. Figure 3.2 depicts the two-body problem in a three-dimensional representation with the z -axis being the energy. The height above the gravitational potential surface is the kinetic energy of the small body. Maximum

kinetic energy occurs at the orbit periapsis and decreases with distance from the large mass. Notice that the total height does not change throughout the orbit, illustrating the fact that its total energy remains constant.

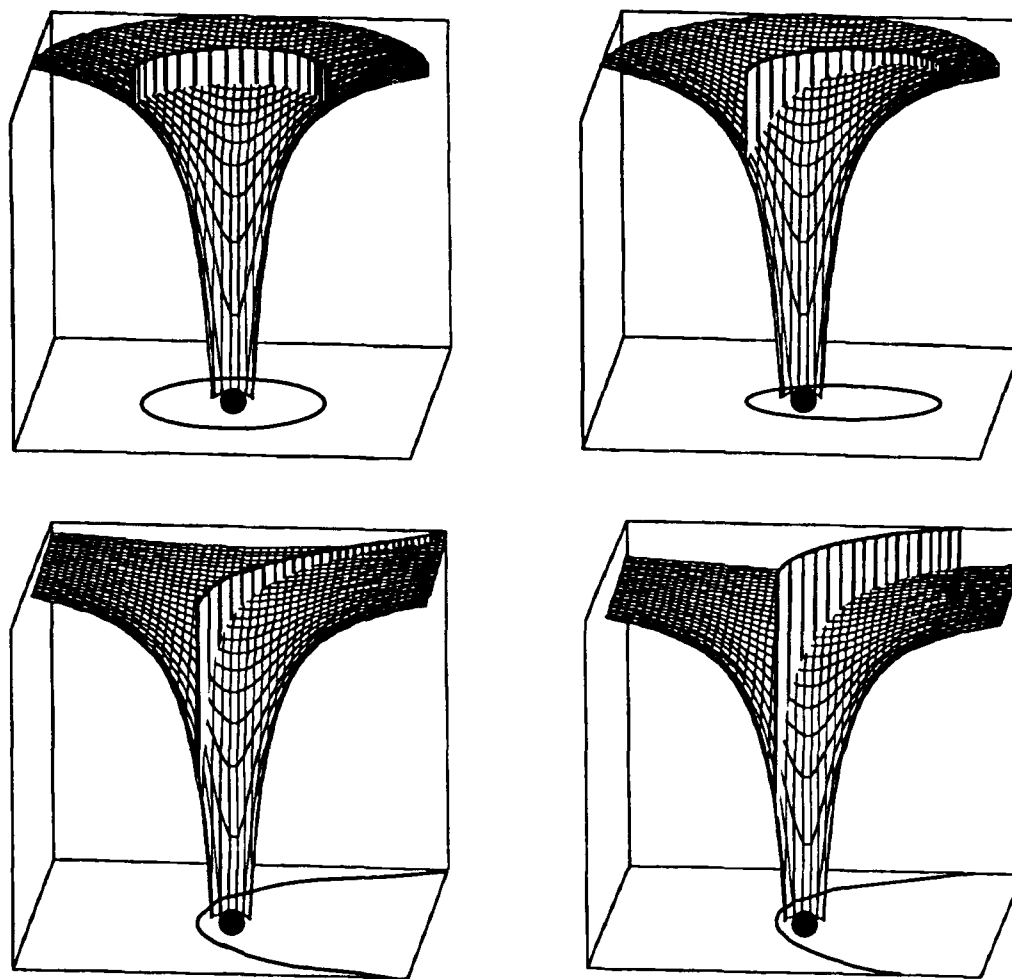


Figure 3.2 Kinetic energy superimposed on the gravitational potential for circular, elliptical, parabolic, and hyperbolic orbits in the two-body problem (Note how the negative total energy in the circular and elliptical cases establishes a circular boundary beyond which lies a region where motion is prohibited. No such region exists for the parabolic or hyperbolic cases).

The potential surface for the circular and elliptical orbits is cut off at a negative level of energy. This establishes a boundary that defines a region where motion is forbidden for a body of that particular energy level. The circular and elliptical examples in figure 3.2 have the same energy and therefore the radius of this boundary is identical. As the eccentricity of the orbit increases, the apogee of the orbit gets closer to the boundary. The boundary can only be reached in a degenerate rectilinear orbit where the velocity goes to zero at the apogee. All points along this boundary are associated with zero velocity because the kinetic energy must go to zero. No such boundary exists for the case with zero or positive total energy. A body that is traveling on a parabolic or hyperbolic trajectory is not prohibited from any area in the plane by this qualitative assessment.

The shape of these boundaries, when they exist, is always circular in the two-body problem. The region outside of the circular boundary is unattainable without increasing the kinetic energy of the mass, such as with a thrusting maneuver for a spacecraft. Once the kinetic energy is increased, the boundary simply moves outward so that the boundary is never violated.

This boundary that divides regions of possible motion and prohibited regions of motion is quite similar in concept to the more complex zero velocity curves of the restricted three-body problem. Understanding the relationship between trajectories to the boundary in the two-body problem makes the limitations of zero velocity curve analysis in the restricted three-body problem much easier to appreciate. Nothing is said about the path that is taken. The boundary merely puts a fence around the area where motion is allowed.

The topology of three-body zero velocity curves take on a much different character than these two-body boundaries because of the rotating reference frame. The zero velocity potential surface is obtained by superposition of the separate potentials arising from static and dynamic forces. Analysis of the potential surface in the restricted three-body problem is the subject of chapter 4. It is of interest, however, to first analyze the purely static gravitational potentials of more than one body before introducing the dynamics of the restricted problem.

3.6 Superposition of Gravitational Potentials

The two-body examples which have been dealt with thus far have assumed that the mass of the orbiting body is negligible. When the mass of the second body is of significant magnitude, the resulting potential surface takes on a very different character than the surface of a single body. Superposition of the two gravity wells leads to a potential surface with an equilibrium saddle forming between the two bodies. This point of equilibrium is located where the gravitational force of the first body is exactly canceled by the second. In analyzing the potential surface, it is apparent that any perturbation from this equilibrium point toward either mass will result in an increasing force toward that same mass, indicating that this point is unstable.

In considering only the force of gravity, the picture is incomplete because dynamic inertial forces are ignored. Because the bodies rotate around each other and are not fixed in space, there are five such equilibrium points in reality, arising from a balance with the centrifugal force. But some interesting information can

be obtained by analyzing the static force relationships between two bodies. Other bodies of significant mass can be superpositioned so that the static gravitational situation of many bodies can be represented in this straightforward technique by superposition of potential wells.

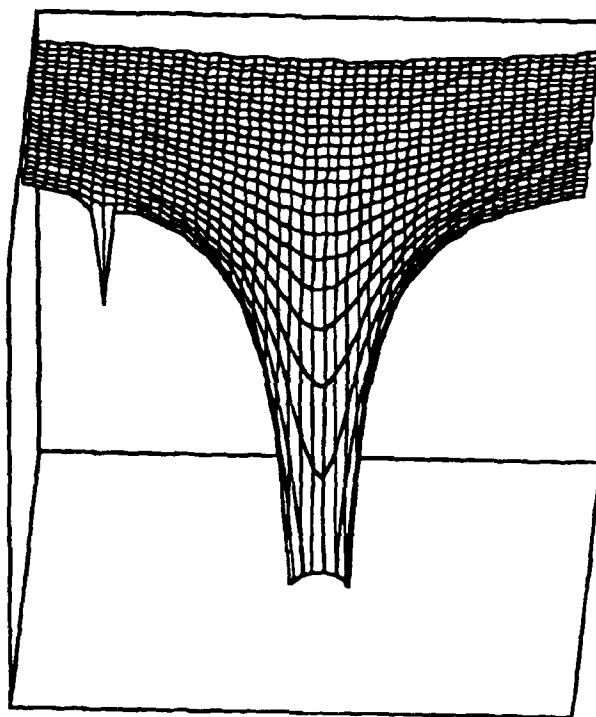


Figure 3.3 Gravity well of the Moon superpositioned on the Earth's potential. Note that the singularity located at the Moon's position does not appear due to the coarseness of the grid.

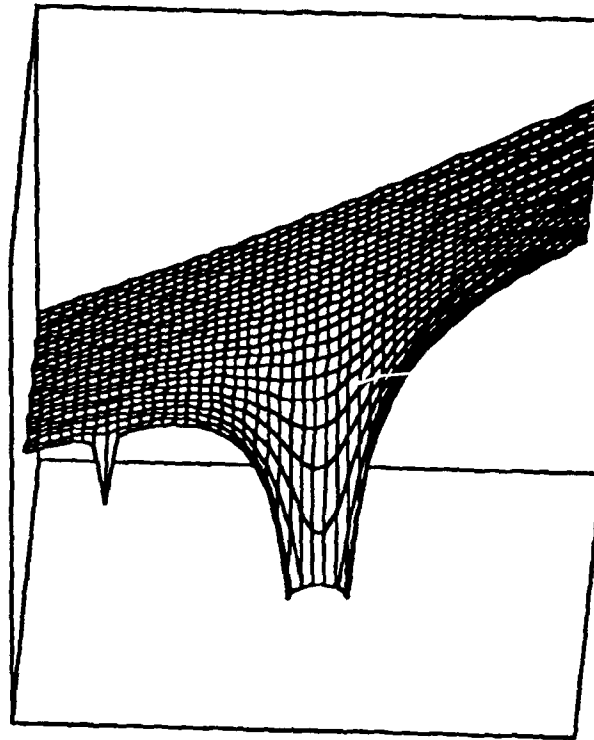


Figure 3.4 Sun's potential superpositioned on the Earth-Moon system. The graph depicts a small section of the Sun's gravity well where the Earth-Moon system is found so that the Sun is located far off the left side of the graph and the energy axis (z -axis) is shifted down (more negative) to expand detail. Notice that the Moon experiences a pull from the Sun that is more than twice as strong as the Earth's pull. Compare to the isolated Earth-Moon system shown in figure 3.3.

It is customary to think that the motion of the Moon is dominated by the gravitational attraction of the Earth. With the Earth as the center of reference, the Moon can be seen to orbit in an ellipse of low eccentricity with minor deviating perturbations. It is perhaps a surprising result to discover that the Moon

experiences a pull from the Sun that is more than twice as great as the gravitational force from the Earth. Figure 3.3 depicts the superpositioned gravity wells of the Earth and Moon in an isolated system.

The situation is dramatically changed when the gravitational attraction of the Sun is included. The Moon is found to be far enough away from the Earth so that it experiences a pull from the Sun that is 2.2 times greater than the Earth's pull. This is depicted graphically in figure 3.4. Although the Moon is considered to orbit the Earth, it would be appropriate to think of the Moon as orbiting the Sun and having its motion perturbed by the Earth. If it were possible to hold the Earth and Sun fixed, the Sun would strip the Moon away. But it is the inertia of the Earth and Moon in their respective orbits about the Sun that keeps the Moon captive in Earth orbit. Their centrifugal force balances with the Sun's gravity so that the system is restored to a potential like that shown in figure 3.3. The resulting two-body motion of the Moon around the Earth is perturbed by the small difference in acceleration from the Sun on the Moon versus the Sun on the Earth. The transition to a rotating coordinate system and the potential due to centrifugal force is covered in the next chapter.

Chapter 4

Derivation of the Potential Function

The potential function of the restricted problem, Ω , was introduced in chapter 2. In this chapter, the zero velocity potential surface will be found through superposition of the component potentials in an effort to help visualize the dynamics of the restricted problem. The shape of the gravitational potential surface generated by the two primary masses is kept unchanged due to the fixed distance of their uniform circular motion. This suggests the use of a rotating coordinate system in which the gravitational force is balanced by the centrifugal force for the orbiting primaries. Understanding the forces that arise from this rotating frame can be a conceptually challenging aspect of the restricted problem.

4.1 Characteristics in a Rotating Reference Frame

In a non-accelerated coordinate system, there are only two types of forces that pertain to the restricted three-body problem. These are Newtonian gravitation and inertia. Gravitation acts externally on a body while inertia is an internal force. Once a rotating reference frame is established, inertia manifests itself in part as the Coriolis force and centrifugal force, both of which take on the appearance of acting externally. The remaining component of inertial force continues to act internally and is associated with the momentum of the body whose velocity is relative to the rotating frame. Since the concept of inertia governs all of these three forces, the term *kinetic* is used to describe the internally acting component of

inertia. The practice of calling the Coriolis force fictitious is counterproductive because the true nature of this force, like that of centrifugal force, is simply inertia. Figure 4.1 summarizes the relationship of forces in the inertial and rotating coordinate systems.

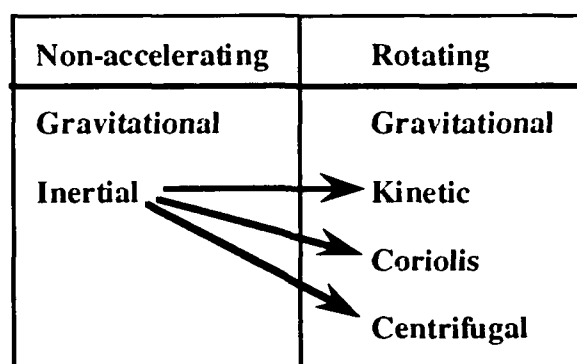


Figure 4.1 Relationship of forces between an inertial and a rotating reference frame. Note that in the non-accelerated reference, inertia is inseparable from kinetic energy and acts internally, while in the rotating frame, inertia manifests itself as external forces as well as the internal force associated with kinetic energy.

When trying to understand the forces that arise in non-inertial reference frames, it can be helpful to mentally switch back to an inertial frame for comparison. As an illustrative example, imagine watching a pottery wheel spin. Say the surface is covered with frictionless ice and a hockey puck is placed on the wheel. The puck will experience no side force and because of its inertia, it will not move from the position from which it was released. From the reference of the

icy platter, however, the puck is traveling in a perfect circle in the direction opposite to the platter's spin. Its velocity relative to the platter is exactly $r \cdot \omega$, its distance from the center multiplied by the angular velocity of the platter. The puck, therefore, has kinetic energy where it had none in the non-accelerated reference. There is no mystery to the force that is attracting the puck so that it maintains its circular path. As readily seen from anyone standing in the room, the Coriolis force and centrifugal force are just manifestations inertia in the rotating frame.

The Coriolis force only acts when there is motion relative to the rotating reference frame. Equations 4.1 relate the x and y components of the Coriolis force to their potential representations:

$$\begin{aligned}\bar{F}_{cor_x} &= -2mn\dot{y}, & U_{cor_x} &= -2mnx\dot{y}, \\ \bar{F}_{cor_y} &= 2mn\dot{x}, & U_{cor_y} &= 2mny\dot{x},\end{aligned}\tag{4.1}$$

where n is the mean motion and the dots denote time derivatives. When a body has zero velocity in the rotating reference frame, \dot{x} and \dot{y} vanish and the Coriolis terms disappear.

Likewise, the kinetic term of $\frac{1}{2}mv^2$ disappears for the zero velocity case.

So the only potentials that are to be considered for a body with zero velocity in the rotating frame for the restricted problem are gravitational and centrifugal.

4.2 The Centrifugal Potential

Similar to the gravitational example that was used in figure 3.1, the centrifugal force can be expressed by its potential function as shown in figure 4.2. Again, the force at any point on the surface is merely the gradient at that point. In a rotating frame, the body experiences this force strictly as a result of its position.

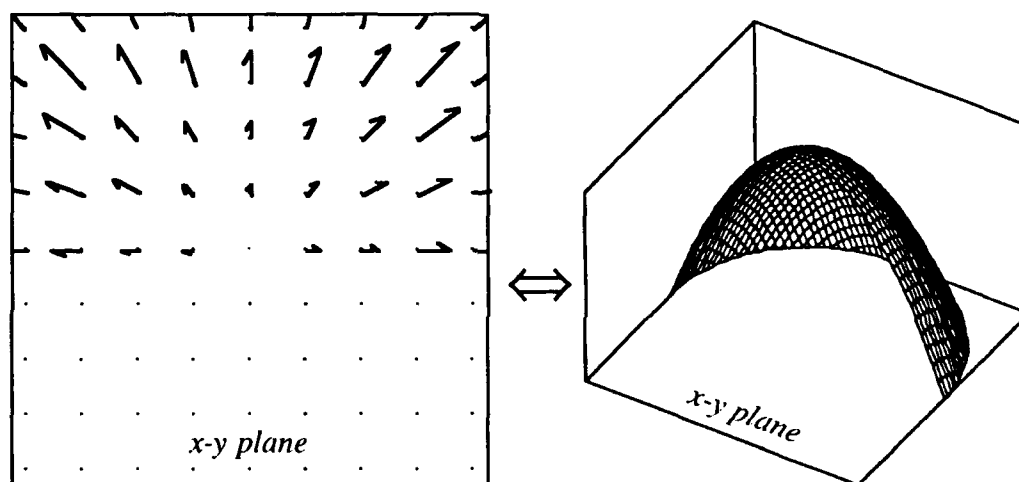


Figure 4.2 Centrifugal force and the corresponding potential of a coordinate system that is rotating about its origin. Force vectors have a one-to-one correspondence to the negative gradient of the surface with energy depicted on the z-axis. Again, half of the field has been cut away for clarity.

Centrifugal force is expressed as:

$$\vec{F}_{cent} = m \frac{v_T^2}{r} \hat{r}, \quad (4.2)$$

where v_T is the tangential velocity and r is the distance from the barycentric origin. The direction of force is away from the origin, as expressed by the radial \hat{r} unit vector. Tangential velocity can be expressed in terms of the average angular velocity, or mean motion, n .

$$v_T = rn. \quad (4.3)$$

Substituting into equation (4.2),

$$\bar{F}_{cent} = m \frac{(rn)^2}{r} \hat{r}, \quad (4.4)$$

and applying the potential relation of equation (3.1), the centrifugal potential is found to be:

$$\begin{aligned} U_{cent} &= - \int mn^2 r \hat{r} \cdot d\bar{r} \\ &= - \frac{mn^2}{2} r^2 \\ &\approx \frac{1}{2} \frac{G(m_1 + m_2)m_3}{l^3} r^2, \end{aligned} \quad (4.5)$$

where Kepler's law:

$$n^2 l^3 \approx G(m_1 + m_2), \quad (4.6)$$

has been used in the last step of equation (4.5) to remove the mean motion term.

The term l in equation (4.6) is the length between the primary masses.

4.3 Superposition of Potentials

The total zero velocity potential surface for the restricted three-body problem is obtained by superposition of the primary gravitational potentials with

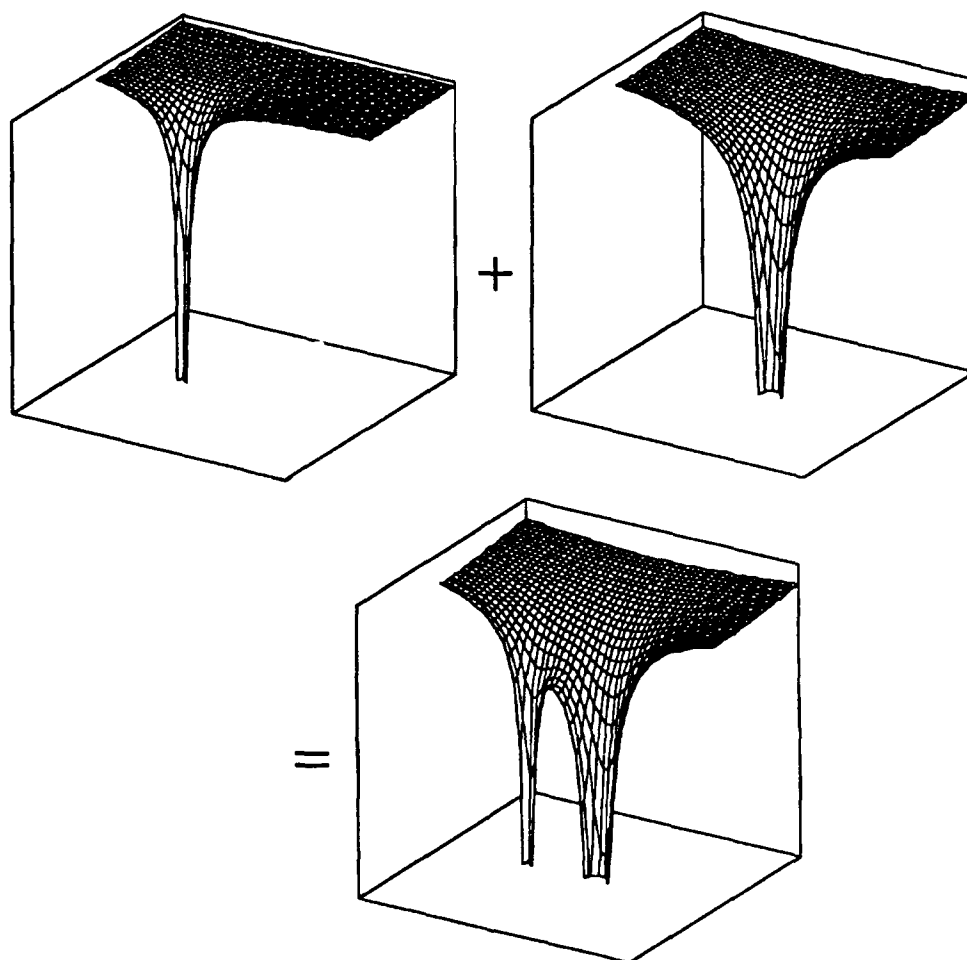


Figure 4.3 Superposition of primary gravity wells (mass parameter $\mu=0.25$)

the centrifugal potential from the rotating frame.

The gravitational potential of the two primaries is given by the superpositioning:

$$\begin{aligned}
 U_{grav_{tot}} &= U_{grav_{m_1}} + U_{grav_{m_2}} \\
 &= -\frac{Gm_1m_3}{r_1} - \frac{Gm_2m_3}{r_2}.
 \end{aligned}
 \tag{4.7}$$

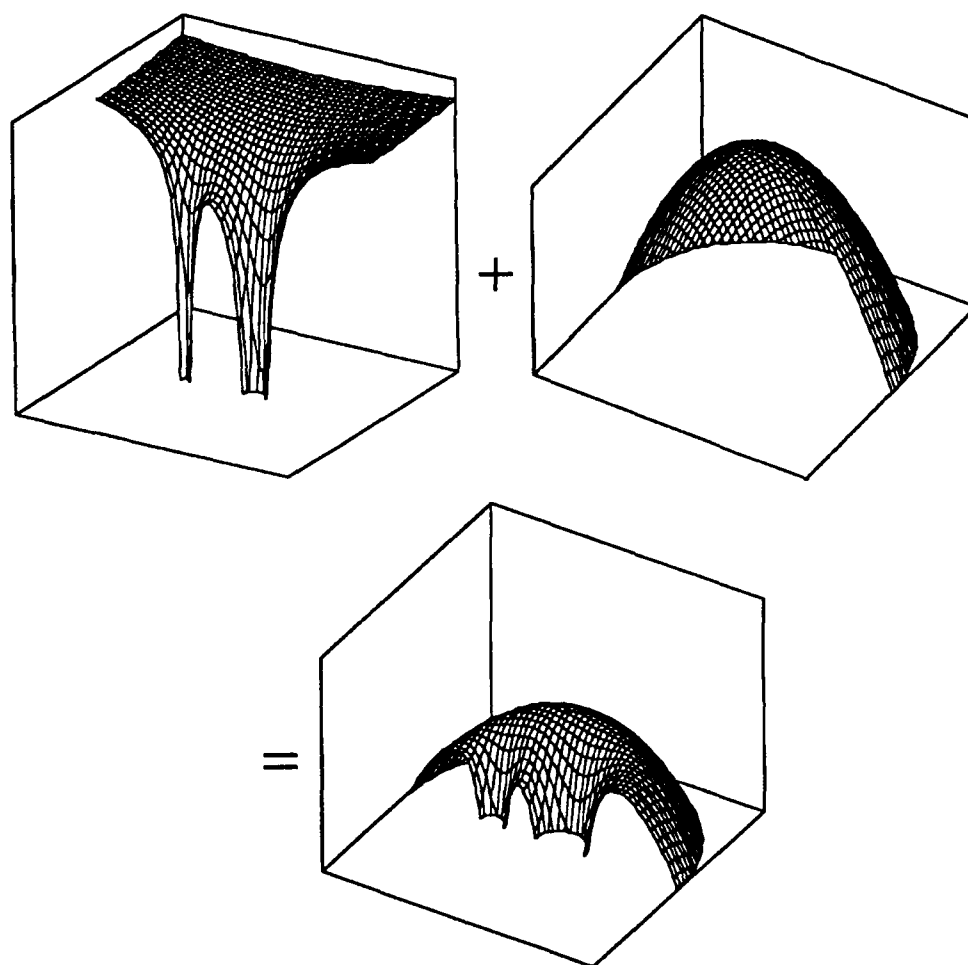


Figure 4.4 Superposition of gravitational potential with centrifugal potential to attain the zero velocity potential surface.

The gravitational potential of the primaries may be superpositioned in the same manner as the static analysis of the Earth-Moon system from chapter 3. While the Earth-Moon system has a mass parameter of $\mu \cong 0.01214$ and the Sun-Jupiter system has a mass parameter of $\mu \cong 0.0009538$, the example in figure 4.3

depicts the case of $\mu=0.25$. The mass parameter is given in equation (4.10) as the ratio of the smaller mass, m_2 , to the total mass. The topology for the surface is essentially the same in all cases except for the limiting case where $\mu=0$ which results in the two-body problem in a rotating frame. The topology will be studied in more detail in chapter 5.

The centrifugal potential is then superpositioned so that equations (4.5) and (4.7) are combined:

$$U_{tot} = -\frac{1}{2} \frac{G(m_1 + m_2)m_3}{l^3} r^2 - \frac{Gm_1m_3}{r_1} - \frac{Gm_2m_3}{r_2}, \quad (4.8)$$

representing the total potential,

$$U_{tot} = U_{grav} + U_{cent}, \quad (4.9)$$

where only gravitational and centrifugal terms affect the potential. The Coriolis and kinetic energy terms do not appear because there is zero velocity relative to the rotating reference frame. So the resulting surface in figure 4.4 is the zero velocity potential surface.

It is then possible to use the basic relationships to put equation (4.8) into non-dimensional form so that the potential function is expressed only in terms of the mass parameter μ .

$$\mu = \frac{m_2}{m_1 + m_2} \quad (4.10)$$

$$1 - \mu = \frac{m_1}{m_1 + m_2} \quad (4.11)$$

The length l is normalized so that the position coordinates of mass m_1 are $(\mu, 0)$ and m_2 are $(1-\mu, 0)$:

$$l = \mu + (1 - \mu) = 1. \quad (4.12)$$

The radius r is the Euclidean norm from the origin to m_3 so that:

$$r^2 = x^2 + y^2. \quad (4.13)$$

The distance r_1 is the distance from mass m_1 to the third mass:

$$r_1^2 = (x - \mu)^2 + y^2. \quad (4.14)$$

Likewise, the distance r_2 is measured from m_1 to m_3 :

$$r_2^2 = (x + 1 - \mu)^2 + y^2. \quad (4.15)$$

Finally, substituting equations (4.10) to (4.16) into equation (4.8), and dividing by the quantity $G(m_1 + m_2)m_3$, the result becomes:

$$\frac{U_{tot} / m_3}{G(m_1 + m_2)} = -\frac{1}{2}(x^2 + y^2) - \frac{(1 - \mu)}{r_1} - \frac{\mu}{r_2}, \quad (4.16)$$

where the right side is recognizable as $-\bar{\Omega}$ from chapter 2.

The zero velocity curves, which were introduced in chapter 2, are seen to be obtained from energy-specific cross sections of the potential function as determined by the Jacobian constant. Zero velocity curves are the subject of the next chapter.

Chapter 5

The Equilibrium Points and Zero Velocity Curves

It was shown in chapter 4 that the potential function is the superposition of the gravitational potential of the two primaries and the centrifugal potential of the rotating reference frame. The equilibrium points and curves of zero velocity are shown to be inseparably related to the potential function.

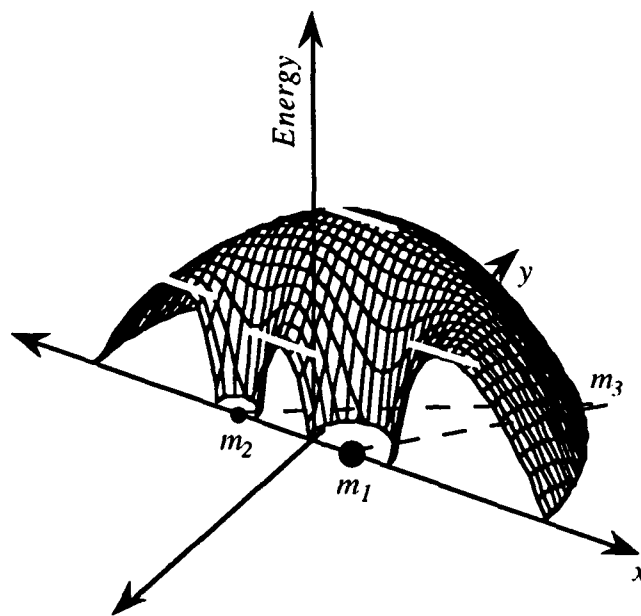


Figure 5.1 Equilibrium points occur where the potential surface has a zero gradient. The plane of motion is found at the energy level determined by the Jacobian constant.

5.1 The Equilibrium Points

There are five points on the potential surface where the gradient is zero. A body located at any of these points will experience zero net force in the rotating frame. They are therefore called equilibrium points and signify a balance between the centrifugal repulsion and gravitational attractions. Sometimes referred to as stationary points or libration points, Lagrange is credited with their discovery in 1772, and in his honor they are popularly called the Lagrange points. His research lead to the discovery of the Trojan asteroids 134 years later [16].

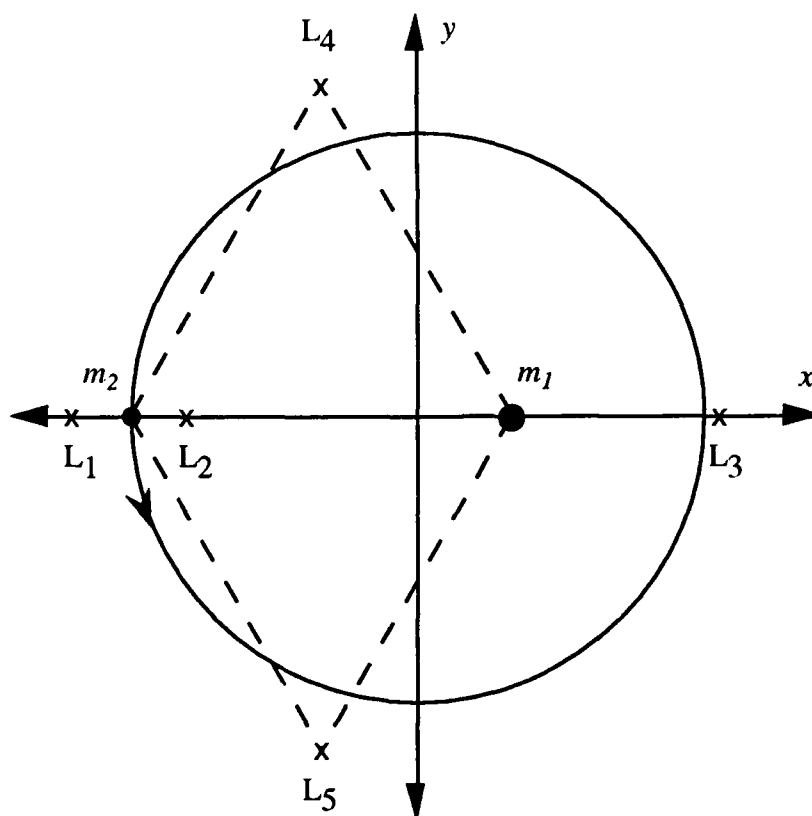


Figure 5.2 The location of the collinear and equilateral Lagrange points in relation to the orbit of the smaller primary mass.

Figure 5.1 shows how the potential surface has a zero gradient at these points. The three points located on the x -axis are known as the collinear equilibrium points and are seen to be saddles. From left to right, these are labeled L_1 , L_2 , and L_3 and their exact location depends on the mass ratio. The other two points, labeled L_4 and L_5 , are found at the top of a potential peak that forms an equilateral triangle with the primaries. The equilateral geometry holds for all values of the mass parameter.

5.2 Zero Velocity Curves

Figure 5.1 also shows the relation of the potential surface to the two spatial dimensions where motion is taking place. The Jacobian constant establishes the height on the z -axis for the plane of motion. The third body may have motion in this plane without penetrating the potential surface.

The height above the potential surface represents energy due to velocity relative to the rotating reference frame. As the third body gets closer to the potential surface, its energy due to velocity decreases. If the body were to come in contact with the surface, it must do so with zero velocity. To get below the potential surface would require negative energy due to velocity. Velocity squared equaling a negative number would correspond to imaginary velocity, therefore it is impossible to penetrate the potential surface.

Zero velocity curves are found by taking a slice through the potential surface at the energy level specified by the Jacobian constant. These curves define regions where motion is possible and where motion is prohibited. If the

region is above the potential surface, then motion is possible. If the region is below the potential surface, motion is prohibited. If the body is found to be contained within a closed contour, it is trapped by the potential surface from all other regions in the plane even though other areas were not strictly energy prohibited. It is impossible to tunnel through the potential surface to get from one permissible region to another.

Figures 5.3 through 5.10 depict a series of zero velocity curves increasing from a low to high energy state. The curves are formed in the x - y plane at the top level of the graph. Although the case $\mu=0.3$ is used, the topology is the same for all values of the mass parameter. Note that the Jacobian constant varies inversely with energy.

Figure 5.3 shows that a body of low energy is captured in the gravity well of one of the primary masses, or if found outside the system, it is prohibited from entering by the centrifugal force of the rotating frame. It is difficult to imagine why a body should be repelled from the primaries. If a body is just sitting out in inertial space with no velocity, it is sure to be attracted into a system of primaries. But such a body, as viewed from the rotating frame, has a great velocity due to its perceived rotation in the direction opposite of the binaries. Its energy in the rotating reference is very high and it is therefore not restricted by the potential surface from entering the primary system. On the other hand, if in the rotating reference a body has low energy due to velocity, it must be moving along with the reference frame so that its own inertia prevents it from entering the primary system.

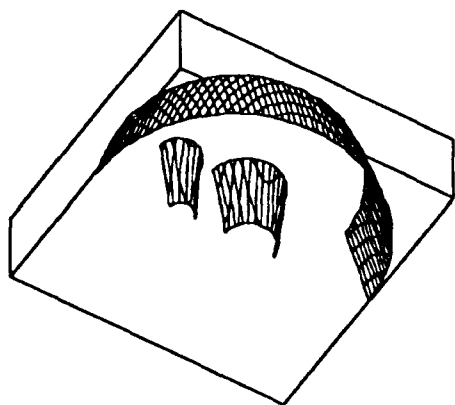


Figure 5.3 Topology for the lowest level has three isolated regions.

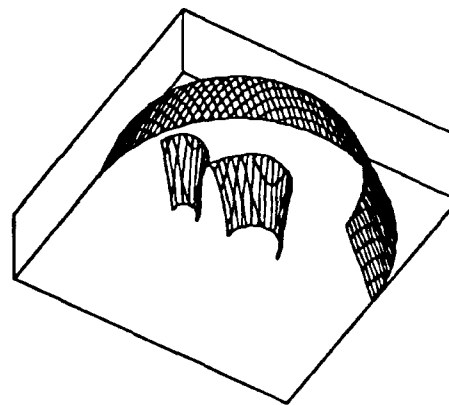


Figure 5.4 Energy level for the L_2 equilibrium point.

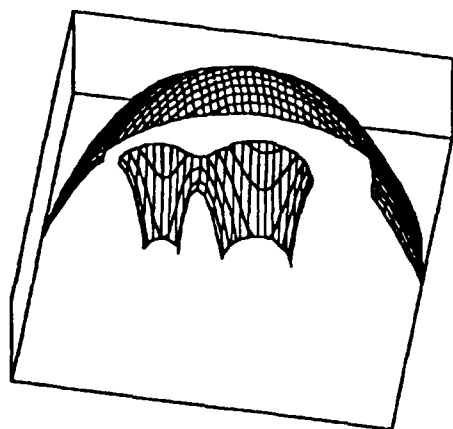


Figure 5.5 Trajectory between the primary masses is not prohibited.

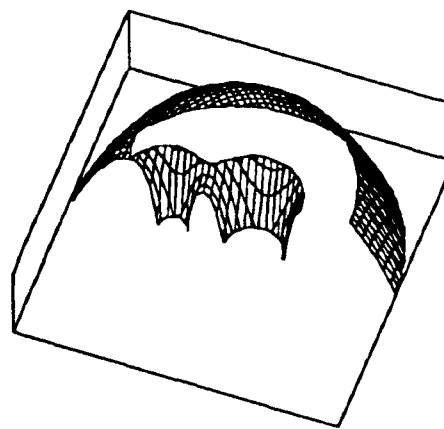


Figure 5.6 Energy level for the L_1 equilibrium point.

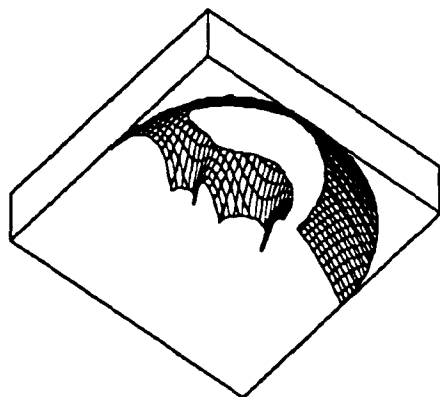


Figure 5.7 Prohibited region is in the shape of a horseshoe.

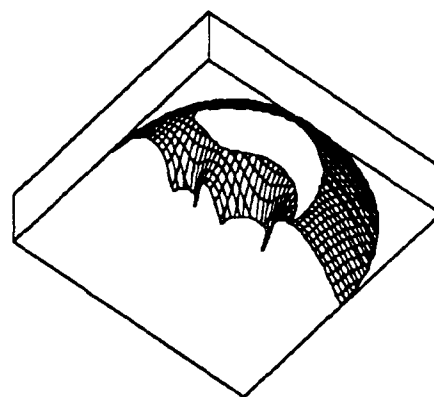


Figure 5.8 Energy level for the L_3 equilibrium point.

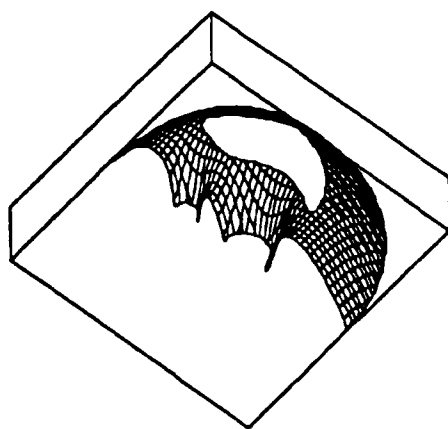


Figure 5.9 Kidney shaped prohibited regions.

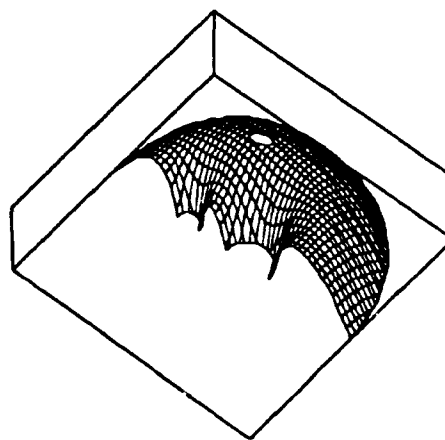


Figure 5.10 Energy level close to L_4 equilibrium point.

The Lagrange points are seen to be located at the energy levels where the topology of the zero velocity curves change. The lowest energy equilibrium point is seen in figure 5.4 to occur at a transition from three regions of possible motion to two. After increasing energy through the L_1 Lagrange point, the two regions become one. The prohibited region shrinks from a horseshoe shape in figure 5.7, through the L_3 point in figure 5.8, to two smaller kidney shaped regions in figure 5.9. The peak of the potential surface is almost reached in figure 5.10. These small ovals are the shape of zero velocity curves near the equilateral Lagrange points. Self-intersecting zero velocity curves are known as *transitional*, while those that do not pass through equilibrium points are known as *typical* [5]. This series of figures should be compared to figure 2.4.

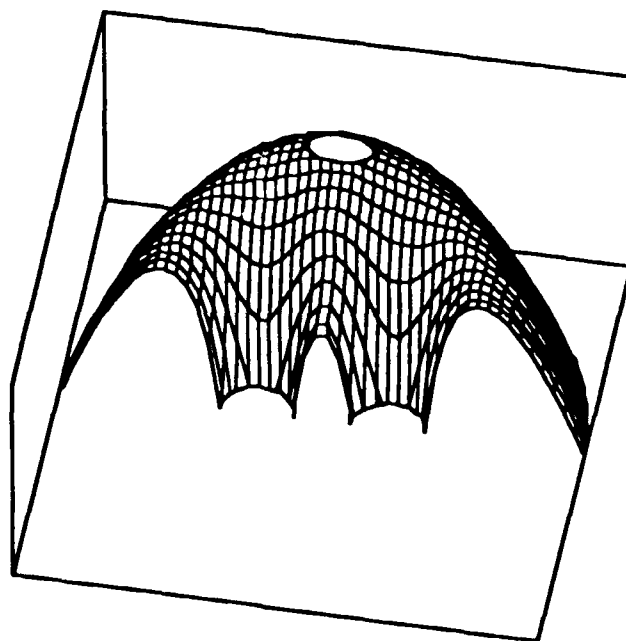


Figure 5.11 Zero velocity curve near the equilateral Lagrange point for $\mu=0.5$.

5.3 Extreme Values of the Mass Parameter

The topology of the potential surface is the same, in general, for all values of the mass parameter. The degenerate case of $\mu=0.0$ and maximum of $\mu=0.5$ are included for completeness. With the mass parameter being defined as the ratio of the smaller mass to the total mass, the largest value it can take is one-half. A symmetry about the x and y axes for the $\mu=0.5$ case in figure 5.11 has given it special attention as the Copenhagen problem [15].

The limiting case of $\mu=0$ is just the two-body problem. Zero velocity curves are seen to take on the shape of concentric circles. The topology is qualitatively different, as evidenced by the equilibrium points becoming a complete circle.

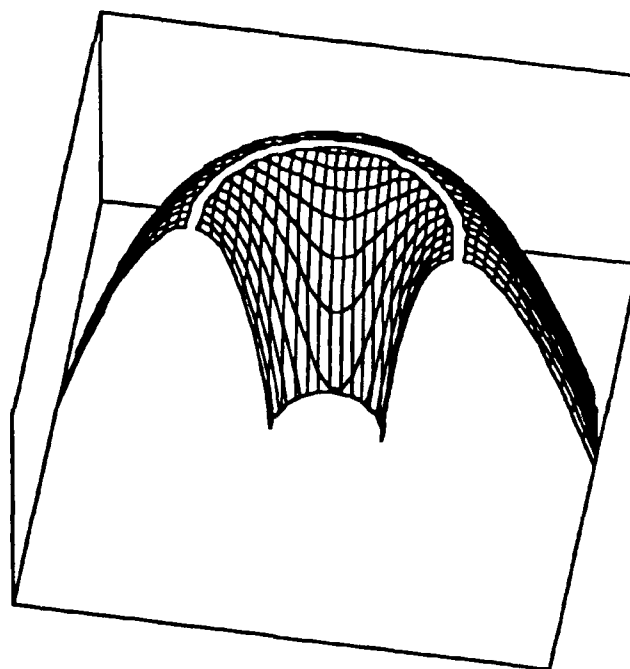


Figure 5.12 Zero velocity curve for $\mu=0$, the two-body problem.

The circular set of equilibrium points shown in figure 5.12 helps to explain the formation of rings around planets. Each point on this ring is known to be stable because it corresponds to a circular orbit.

For the regular three-body potential surfaces, the collinear points are highly unstable. It would seem more difficult for a body to remain on top of a peak than in a saddle, but the equilateral points are stable if $\mu < 0.0385$ [15]. Although it is not usual for a peak in potential to be stable, the Coriolis force acts against deviations to maintain position at the peak.

5.6 Applications for the Earth-Moon System

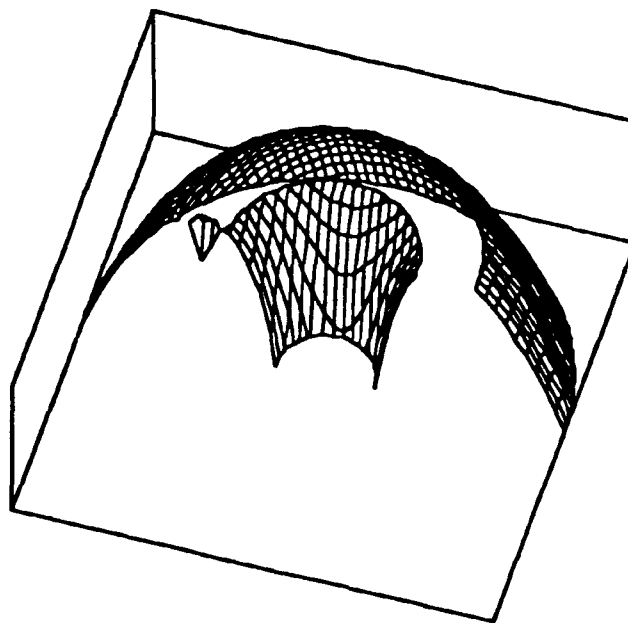


Figure 5.13 The cis-lunar Lagrange point ($\mu=0.0121$).

The most practical application of the restricted three-body problem from an engineering standpoint belongs to the Earth-Moon system. Launching a rocket into orbit may be thought of, in terms of energy, as climbing up Earth's gravity well. When going to the Moon, it is very inefficient to land any mass that is only needed for the return trip. Were it not for the Lunar Orbit Rendezvous (LOR) profile, the Apollo program would have required a rocket much larger than the Saturn V which, like the Russian's effort, might never have gotten off the ground. It is interesting to note how the figure-8 trajectories used in the Apollo missions relate to the zero velocity curve that appears in figure 5.14

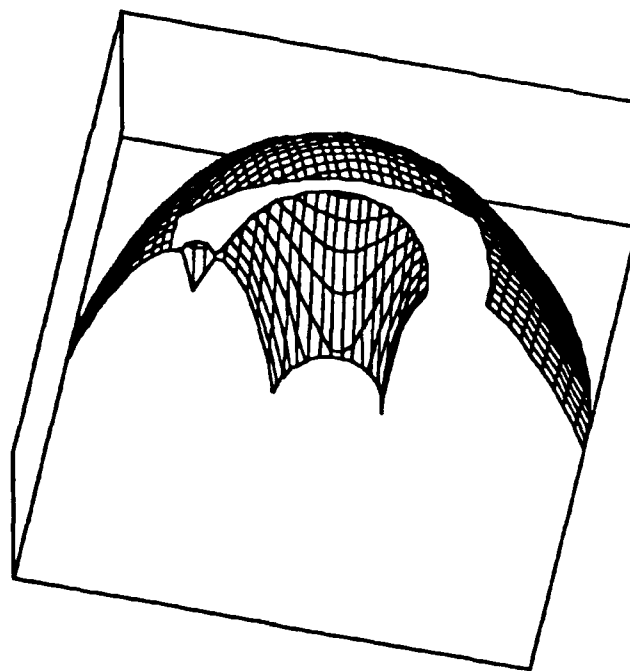


Figure 5.14 The trans-lunar Lagrange point ($\mu=0.0121$).

Despite its energy efficiency, the LOR profile is restrictive because of the constraints imposed by the rendezvous. Landing sites need to be located near the lunar equator. If not, a lunar launch window has to be met in order to prevent a costly plane change maneuver. A base located at mid-latitude would have a launch window open every 14 days as the Moon rotates 180° underneath the rendezvous orbit. This restriction is referred to as the mid-latitude accessibility constraint [6].

The collinear Lagrange points L_1 and L_2 are being considered as the location for a future space station. Operations to any point on the lunar surface could be accomplished without the launch window restrictions that LOR faces. Although the points are not naturally stable, orbits in the vicinity of the equilibrium points can be maintained with an acceptable expenditure of station-keeping thrust.

The trans-lunar point is beyond the Moon by several lunar diameters. An orbit around this point looks like a halo because the spacecraft appears at the edge of the Moon's outline when viewed from the Earth. Such a halo orbit would be ideal for a communication link with any lunar operation conducted on the far side of the Moon. The cis-lunar point, located between the Moon and Earth, is the most accessible from low Earth orbit because of its low energy potential. It is also the closest equilibrium point to the Earth. With the possibility of mining the Moon for rocket fuel, the cis-lunar point would be a very efficient staging base for sustained missions to Mars. Exploitation of the Lagrange points will make future space operations more efficient.

Chapter 6

Summary

The superposition analysis in a three-dimensional representation clearly reveals the component forces of the restricted problem. For the case where the third body has zero relative velocity, the only forces that influence the potential are due to the gravitational attraction of the primary masses and the centrifugal effect of the rotating reference frame. These define a potential surface and any velocity that the third body possesses manifests itself as energy above the surface.

Zero velocity curves as well as the Lagrange points have been shown to be contained within the potential surface through special relationships. The zero velocity curves are intersections of the potential surface at the energy level determined by the Jacobian constant of the third body. They define regions where motion is possible and motion is prohibited. The Lagrange points are located at the five points where the gradient of the surface goes to zero. This occurs at the levels of energy where transitional zero velocity curves are found and the topology changes. The collinear equilibrium points are located at saddles and, although useful halo-type orbits can be maintained around them, they are unstable points. The equilateral points are at the highest level of energy on the potential surface. In the case where the mass ratio of the primaries is small, these points are stable.

The restricted problem of three bodies forms a good approximation for real-world situations. Lagrange's calculation of equilibrium points was thought to

be a mathematical quirk of no real significance. The subsequent discovery of the Trojan asteroids is an example where theory was ahead of experiment by over 100 years. Rendezvous and control of spacecraft in orbit about the collinear equilibrium points is a current topic of research. It is the destiny of mankind to return to the Moon, venture on to Mars and beyond. Exploitation of the Lagrange points will make these endeavors more cost effective.

Bibliography

- [1] Danby, J. M. A.: 1962, *Fundamentals of Celestial Mechanics*, The Macmillan Co., New York.
- [2] Euler, L.: 1772, *Theoria Motuum Lunae*, Typis Academiae Imperialis Scientiarum, Petropoli.
- [3] Faintich, M. B.: 1973, "Three-Dimensional Zero Velocity Contours", *Celestial Mechanics*, **8** (1973) 291-296.
- [4] Farquhar, R. W.: 1971, *The Utilization of Halo Orbits in Advanced Lunar Operations*, NASA Technical Note D-6365.
- [5] Goudas, C.L., Leftaki, M. and Persagourakis, E. G.: 1990, "Motions in the Field of Two Rotating Magnetic Dipoles. III: Zero-Velocity Curves and Surfaces", *Celestial Mechanics*, **47** (1990) 1-14.
- [6] Haynes, D. A.: 1991, "Libration Point Staging for SEI Lunar Missions: Station Keeping Implications", *Advances in the Astronautical Sciences*, Vol **76**, Part III, 1921-1933.
- [7] Hill, G. W.: 1878, "Researches in the Lunar Theory", *Am. J. Math*, **1** (1878) 5, 129, 245.
- [8] Jacobi, C. G. J.: 1836, "Sur le mouvement d'un point et sur un cas particulier du problème des trois corps", *Comptes Rendus*, **3** (1836) 59.
- [9] Jones, B. L. and Bishop, R. H.: 1993, "Stable Orbit Rendezvous for a Small Radius Trans-lunar Halo Orbit," Presented at the 1993 AAS/AIAA Space Flight Mechanics Meeting, AAS Paper 93-144, Pasadena, CA, Feb 22-24, 1993.
- [10] Lagrange, J.: 1867-92, "Œuvres" (M. J.-A. Serret, ed.), 14 vols. Gauthier-Villars, Paris.
- [11] Lundberg, J., Szebehely V., Nerem, R. S. and Beal, B.: 1985, "Surfaces of Zero Velocity in the Restricted Problem of Three Bodies", *Celestial Mechanics*, **36** (1985) 191-205.
- [12] *Pioneering the Space Frontier*: 1986, The Report of the National Commission on Space, Bantam Books, New York.

- [13] Poincaré, H.: 1892-99, *Les Methodés Nouvelles de la Méchanique Célèste*, Gauthier-Villars, Paris, Vol 3.
- [14] Roy, A. E.: 1978, *Orbital Motion*, Adam Hilger Ltd., Bristol.
- [15] Szebehely, V. G.: 1967, *Theory of Orbits*, Academic Press, New York,.
- [16] Szebehely, V. G.: 1989, *Adventures in Celestial Mechanics*, University of Texas Press, Austin, Texas.
- [17] Szebehely, V. G.: 1990, "Chaos, Stability and Predictability in Newtonian Dynamics", *Predictability, Stability, and Chaos in N-Body Dynamical Systems* (A. E. Roy, ed.), NATO ASI Series B: Physics Vol 272, 63-71.
- [18] Torby, B. J.: 1984, *Advanced Dynamics for Engineers*, Holt, Rinehart and Winston, New York.
- [19] Wintner, A.: 1941, *The Analytical Foundations of Celestial Mechanics*, Princeton University Press, Princeton, New Jersey.

Vita

Christopher Mark Thomas Tuason was born on August 11, 1964 in Evanston, Illinois, the son of Dr. Roman Viado Tuason, Jr. and Kcenia Cornelia Artymiak. In 1982, after completing his work at Bridgmont High School in San Francisco, California, he entered the United States Air Force Academy. In 1986, he was commissioned an officer and graduated with a Bachelor of Science in Electrical Engineering with a double major in physics. Since graduation from the Air Force Academy, he has completed several flight training courses as an instructor navigator and pilot in fighter-bomber aircraft. In 1991, he was selected by the Air Force Institute of Technology to pursue a masters degree in aerospace engineering and in the following January he entered The Graduate School of The University of Texas at Austin. He is married to the former Lisa Maria Farthing who gave birth to their first child, Christiana Maria, in November 1992.

Permanent address: 1381 Brussels Street
San Francisco, CA 94134

This thesis was typed by the author using Microsoft Word 5.0 for the Macintosh.